Short-Term Scientific Mission report

Numerical simulations of single-joints for CLT structures under monotonic and cyclic conditions

Grantee:
Matteo Izzi, Ph.D. Candidate, Research Assistant
University of Trieste and CNR IVALSA Trees and Timber Institute

Host:
Gerhard Schickhofer, Professor, Head of Institute
Institute of Timber Engineering and Wood Technology, Graz University of Technology

In collaboration with:
Georg Flatscher, Ph.D. Candidate, Research and Teaching Associate
Institute of Timber Engineering and Wood Technology, Graz University of Technology

Ph.D. Supervisor:
Massimo Fragiacomo, Associate Professor
Department of Architecture, Design and Urban Planning, University of Sassari

Ph.D. Co-Supervisor:
Giovanni Rinaldin, Ph.D., Research Fellow
Department of Architecture, Design and Urban Planning, University of Sassari

Institute of Timber Engineering and Wood Technology
Graz University of Technology, Graz, Austria
March 01, 2015 – May 31, 2015

1 PREVIOUS COLLABORATIONS WITH THE HOSTING INSTITUTE

The grantee was hosted at the Institute of Timber Engineering and Wood Technology, Graz University of Technology, between November 2014 and January 2015 for a STSM financially supported by COST FP1004. Within the previous collaboration, an extensive experimental programme was carried out on Simpson Strong-Tie annular ringed shank nails. Monotonic and cyclic shear tests in parallel and perpendicular direction to the face lamination of a CLT panel, and withdrawal tests, investigated the bearing capacity of a nail driven in the plane side of a CLT element. Furthermore, uniaxial tension tests and bending tests were performed on single fasteners to determine the ultimate tensile strength and the yielding moment, respectively. The current STSM, financially supported by COST FP1402, was focused on the results of the monotonic tests; mean and characteristic values of the mechanical properties were assessed following the procedures of EN 12512 and compared with the simplified calculation methods provided by the standards. Moreover, monotonic and cyclic mechanical tests were simulated on finite element models of single joints used in cross-laminated timber (CLT) buildings to anchor typical metal connectors to the timber panels.

2 INTRODUCTION

The development of seismic resistant multi-storey timber buildings made of cross-laminated (CLT) panels was the challenge of the last few years. Due to the high in-plane stiffness and the linear-elastic behaviour of the timber panels, the dynamic response of CLT buildings is strongly influenced by the connections used. The hysteretic behaviour of single-joints and CLT wall systems was the focus of several experimental testing programmes. Shear and pull-out tests investigated the performances of typical metal connectors (such as hold-downs and angle brackets) and screwed panel-to-panel connections (Bratulic *et al.* 2014; Flatscher *et al.* 2014a-b; Tomasi and Smith 2014; Gavric *et al.* 2015a-b). Moreover, significant energy dissipation was demonstrated by racking tests performed on CLT walls with several layouts of connections and openings (Ceccotti *et al.* 2006; Hummel *et al.* 2013; Gavric *et al.* 2015c) and with full-scale shaking table tests (Lauriola and Sandhaas 2006; Ceccotti 2008; Ceccotti *et al.* 2013; Flatscher and Schickhofer 2015).

Linear or dynamic static analyses are commonly used by practicing engineers to evaluate the seismic load-carrying capacity of CLT walls or sub-assemblies. A more accurate prediction of the seismic load-carrying capacity can be obtained with non-linear static analyses, which provide more realistic capacity curves and allow the definition of the Limit States. A typical pushover loading scheme of a CLT wall is depicted in Figure 1. The CLT wall is restrained to a rigid foundation, schematized by a metal beam, with hold-downs and angle brackets. Annular ringed shank nails anchor the metal connectors to the CLT wall, while threaded bolts connect the same elements to the foundation. A stiff element, restrained on top of the wall to simulate the effect of the upper floor, is used to apply both vertical and horizontal loads. The main load-carrying direction is shear for the angle brackets and tension for the hold-down (axial direction), however it was shown by Gavric *et al.* (2015a) that the angle brackets affect the behaviour of the wall providing a significant contribution also in their weaker (axial) direction.

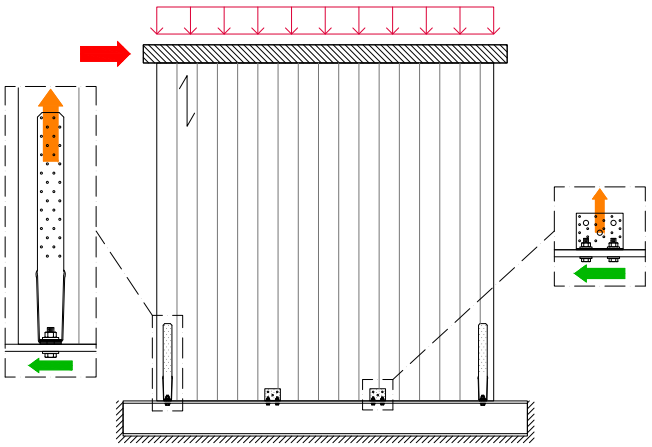

Figure 1. CLT wall system with pushover loading scheme,
and enlargement of a hold-down (left) and angle bracket (right).

Predicting the behaviour of metal connectors is crucial to determine the performances of CLT wall systems; a capacity based design method at the connection level was proposed by Gavric *et al.* (2013). As discussed also in Gavric *et al.* (2015a), the metal connectors must be designed with thick sections to avoid undesired brittle failures and ensure nail plasticization. Ductility in the connector metal part is generally lower than in the nailed steel-timber connection; moreover, failure of a metal connector increases stresses in the other connectors, leading to a potential failure for loss of equilibrium.

Determining the load-carrying capacity of connections made with dowel-type fasteners in CLT is relatively difficult compared to traditional sawn timber or structural composite lumber. An analytical model to predict the fastening capacity was developed by Uibel and Blaß (2006, 2007); specific rules for connections made in CLT were included in the ÖNORM B 1995-1-1 (Austrian National Annex of Eurocode 5, 2014). However, design formulas were not included in structural design codes of any other European country.

The experimental programme described herein was aimed at improving the knowledge on the behaviour of typical connections used in CLT buildings, by investigating the performances of Simpson Strong-Tie annular ringed shank nails (also referred to as connector nails). These nails are used to connect hold-downs and angle brackets to the CLT wall. Shear tests in parallel and perpendicular direction to the face lamination of the CLT panels, and withdrawal tests, were carried out on nails driven in the plane side of the CLT panels. Furthermore, tension tests and bending tests investigated, respectively, the tensile strength and the yielding moment of the nails. The mechanical properties were assessed in terms of strength, stiffness and ductility as prescribed in EN 12512:2001/A1 (2005); characteristic values of the experimental strength capacities were derived according to EN 14358 (2006), and were compared with the formulations provided by the reference standards (EN 1995-1-1:2004+A2 2014, also referred to as Eurocode 5; ETA 04/0013 2013; ÖNORM B 1995-1-1 2014).

A numerical model of a nail driven into a CLT element is subsequently introduced and calibrated on the experimental results. In the model, the shear and withdrawal behaviour of the connection were modelled using newly developed non-linear spring elements (Rinaldin *et al.* 2013). As an applicative example, shear and tension tests were simulated on a Finite Element (FE) model of a Simpson Strong-

Tie AE116 angle bracket (ETA 06/0106 2013), and the results were compared with analogous setups tested by the holz.bau forschungs gmbh.

3 EXPERIMENTAL SETUPS AND LOADING PROTOCOLS

The experimental programme investigated the performances of an annular ringed shank nail of length L = 60 mm and outer diameter d = 4 mm (ETA-04/0013 2013, Figure 2-left) produced from a cold-formed steel wire. The threaded cylindrical shank increases the pull-out resistance, while the conical-shaped cap improves the clamping to the metal plate and enforces a failure mode with two plastic hinges also when connected to thin metal plates (failure mode called "*e*" in Eurocode 5 2014).

Various five-layered CLT panels with a thickness of 134 mm (**26**-28-**26**-28-**26**, Figure 2-right) were used in the tests. The numbers in brackets denote the thickness of each board layer; the bold notation was used to mark the layers with boards parallel to the face lamination of the panel. Timber boards with strength class C24 were used to produce the CLT panels; in accordance with EN 1380 (2009), the panels were conditioned at 20°C temperature and 65% relative humidity before performing the tests.

Figure 2. Simpson Strong-Tie annular ringed shank nail (left) and CLT specimens used for withdrawal tests (right).

Five uniaxial tension tests and ten monotonic bending tests were performed on single fasteners to determine, respectively, the ultimate tensile strength and the moment-rotation relationship of the fastener. The tension tests were carried out with displacement control until failure; as shown in Figure 3-left, a thin metal pipe was placed around the nail shank to increase the clamping to the testing machine.

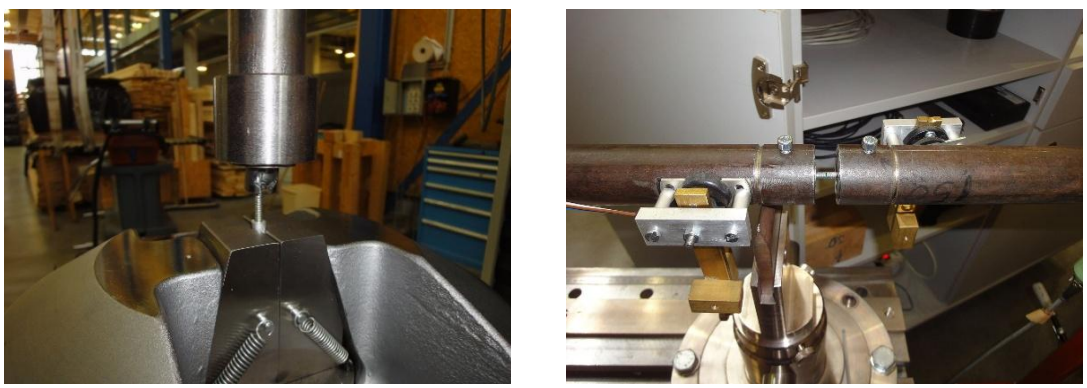

Figure 3. Experimental setup for tension tests (left) and bending tests (right).

The experimental setup adopted for the bending tests was similar to the configuration depicted in Appendix A of EN 409 (2009). Tests were performed with displacement control until 45°, assuming a free bending length of three times the diameter (12 mm, see Figure 3-right).

Six shear tests were carried out in parallel and five in perpendicular direction to the face lamination of the CLT panels. A symmetric system was adopted (Figure 4), with two nails driven at the same location in the opposite plane sides of the CLT panel (EN 1380 2009). The load was applied to the nails cap with two metal plates of 4 mm thickness, obtained by cutting the shoulders of two hold-downs. To minimize the initial friction between the metal plates and the timber surfaces, thin metal blades were interposed among those elements while driving the nails into the panel and removed before testing. EN 26891 (1991) was used to define the loading protocol of the shear tests, assuming an estimated maximum load of 9.0 kN (4.5 kN for each nail). Load control with an input force rate of 1.8 kN/min was used up to 70% of the estimated maximum load; displacement control at a rate of 4 mm/min was used afterwards.

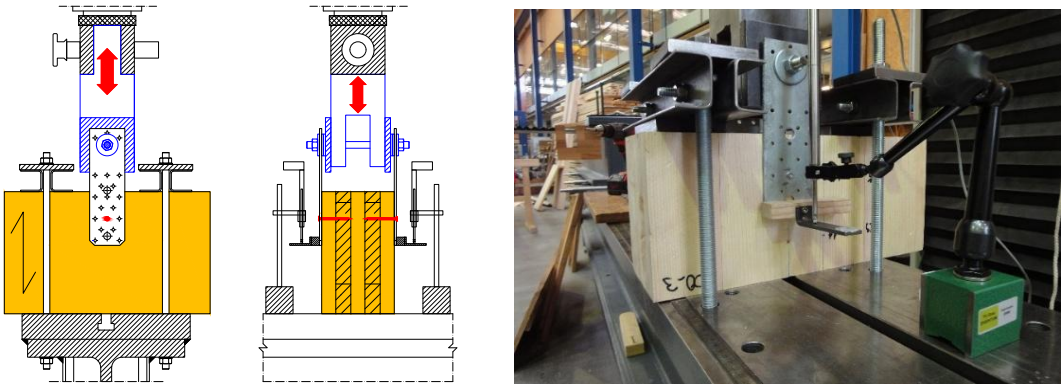

Figure 4. Experimental setup for shear tests (left: front view, centre: side view, right: photo).

Withdrawal tests were carried out with displacement control at a rate of 2 mm/min; tests were stopped after a 40% loss of the maximum bearing capacity; twenty-two connections were tested within this series, with a nail driven in the plane side of a CLT panel (Figure 5).

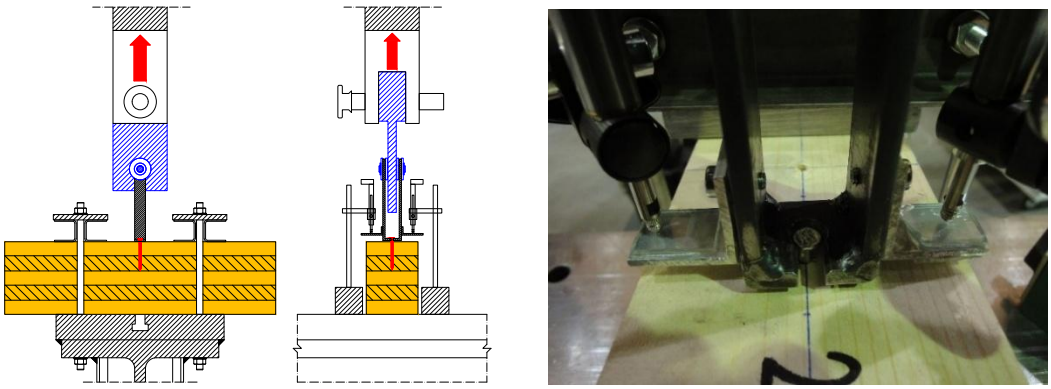

Figure 5. Experimental setup for withdrawal tests (left: front view, centre: side view, right: photo).

Measurements of moisture content (MC) and density were taken either in the proximity (shear tests) or in correspondence (withdrawal tests) of the nail location in the tests (Figure 6). Mean and characteristic values at 12% MC were defined in accordance with EN 384 (2010).

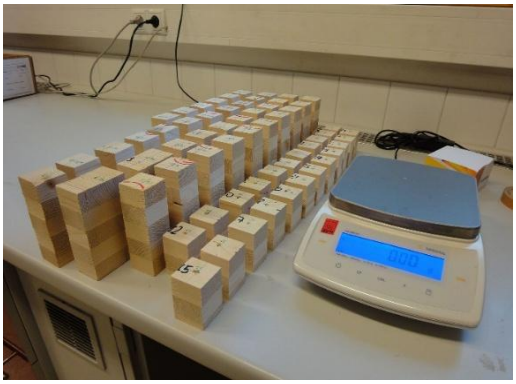

Figure 6. Samples used to determine moisture content and density of the CLT panels.

4 EXPERIMENTAL TEST RESULTS AND DISCUSSIONS

Mean values and coefficients of variation (x_{mean} and COV) of the mechanical properties were assessed following the procedures given by EN 12512:2001/A1 (2005). Characteristic values (x_{char}) were defined in accordance with EN 14358 (2006) and compared with the analytical models provided by the reference standards (Eurocode 5 2014; ETA-04/0013 2013; ÖNORM B 1995-1-1 2014). The subscripts 05 and 95 were employed to denote the 5th and 95th percentile of the statistical distribution.

4.1 Tension and bending tests of the nails

The mechanical properties obtained from the tension tests of the nails are listed in Table 1, while Table 2 presents the characteristic tensile strength. All the tests showed a brittle failure in the core section of the shank after few millimetres of elongation (Figure 7). The tensile strength of the nail f_u was defined by the ratio between the maximum load N_{max} and the core section area, with diameter d' = 3.6 mm (ETA-04/0013 2013).

Figure 7. Failure modes of the uniaxial tension tests.

Table 1. Mechanical properties of nails in tension tests.

Property	x_{mean}	COV
f_u [N/mm^2]	892.22	0.81%

Table 2. Characteristic tensile strength of the nail.

Property	x_{char}
$f_{u,05}$ [N/mm^2]	788.93
$f_{u,95}$ [N/mm^2]	1008.97

The tensile capacity obtained multiplying $f_{u,05}$ by the core section area (8.0 kN) is slightly higher than the corresponding value defined in the ETA-04/0013 (2013), equal to 7.5 kN. It must be noted that Eurocode 5 (2014) and ETA-04/0013 (2013) suggest a tensile strength $f_{u,k}$ = 600 N/mm^2, while the experimental $f_{u,05}$ is 31% higher.

EN 409 (2009) states that the yielding moment $M_{y,Rk}$ must be assumed either as the peak value of the moment-rotation relationship, or as the moment associated to the ultimate rotation. Based on some issues with the experimental setup, the mechanical properties of the bending tests (Table 3) were assessed with an ultimate rotation of 40° instead of the 45°.

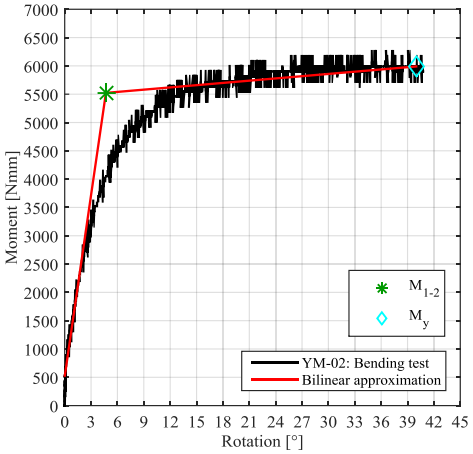

Figure 8. Moment-rotation relationship and bilinear approximation of a nail bending test.

A typical moment-rotation relationship (black line) and the bilinear approximating curve (red line) are displayed in Figure 8. The bilinear schematization was chosen as a simple moment-rotation relationship to be used in numerical simulations. The elastic stiffness was defined as the secant line between 10% and 40% of the maximum moment (EN 12521 2001), while the inelastic branch was set as the secant line between the points at 20° and 40° of rotation. The symbols $M_{1\text{-}2}$ and $\varphi_{1\text{-}2}$ were used to define the intersection point between elastic and inelastic branches, while the bending moment associated to the ultimate rotation (40°) was labelled as M_y.

Table 3. Mechanical properties of nail bending tests.

Property	x_{mean}	*COV*
$\varphi_{1\text{-}2}$ [°]	3.69	27.58%
$M_{1\text{-}2}$ [Nmm]	5258.39	11.86%
M_y [Nmm]	6042.84	12.26%

Table 4. Characteristic yielding moment of the nail.

Property	x_{char}
$M_{y,05}$ [Nmm]	4599.72
$M_{y,95}$ [Nmm]	7827.60

Compared with the ultimate tensile strength of Table 1, the yielding moment of the nail shown in Table 3 is characterized by a higher *COV*. The residual stresses produced by cold forming might

have influenced the behaviour in bending of the nails; moreover, results might be affected by the limited number of tests performed.

As visible in Figure 9, plastic hinges were fully developed only on some test specimens, while others showed a partially developed plastic hinge and a distributed plastic deformation. Signs of failure were not visible in any test specimens.

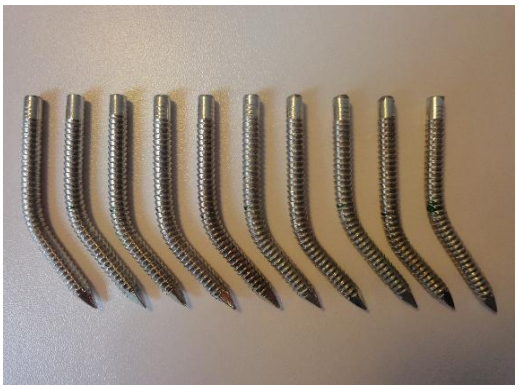

Figure 9. Deformed fasteners after bending tests.

The characteristic yielding moment $M_{y,05}$ (Table 4) was compared in Table 5 with the analytical models provided by the reference standards and literature. The first model (Case *I* in Table 5: Eurocode 5 2014; ETA-04/0013 2013; ÖNORM B 1995-1-1 2014) was derived for a dowel-type fastener with smooth shank and defines the yielding moment depending upon the ultimate tensile strength $f_{u,k}$ = 600 N/mm^2 and the outer diameter d:

$$M_{y,Rk} = 0.3 f_{u,k} d^{2.6} \tag{1}$$

To account for the threaded shank and the uncertain position at which the plastic hinge was developed, an alternative formulation of Equation (1) was also considered (Case *II*), in which the outer diameter d was replaced by the core diameter d'. The second model (Case *III* in Table 5: Ehlbeck and Larsen 1993) adopts a fully plastic approach and defines the yielding moment as shown below:

$$M_{y,Rk} = f_{y,k} d'^3 / 6 \tag{2}$$

where $f_{y,k}$ is an "equivalent" yielding tension, estimated as 80% the ultimate tension of the axial tests $f_{u,05}$, and d' is the core diameter.

Table 5. Comparison of characteristic experimental results and analytical values: Bending tests of nails.

Case	$f_{u,k}$ $\left[\text{N/mm}^2\right]$	d $\left[\text{mm}\right]$	$M_{y,k}$ $\left[\text{Nmm}\right]$	$\frac{M_{y,k}}{M_{y,05}}$
I	600	4.0	6616.50	1.44
II	600	3.6	5031.05	1.09
III	631	3.6	4907.78	1.07

The analytical model prescribed in the reference standards (Case *I*) provided an analytical value significantly higher than $M_{y,05}$. Differences between the same model and the experimental value

reduced to 9% by substituting d' to d (Case *II*), however the best agreement was shown in Case *III* where the "equivalent" yielding tension was used.

4.2 Withdrawal and shear tests of the nails

Mean and characteristic values of density at 12% MC (ρ_{glob} in Tables 6-7) were determined from thirty-two samples taken in proximity of the nail location in the tests, assuming a standard normal distribution. Twenty-two samples were cut from the withdrawal tests, whereas five samples were considered for each series of shear tests. The same quantities were also defined within each test series (respectively ρ_{withdr}, $\rho_{sh\text{-}0°}$, $\rho_{sh\text{-}90°}$).

Table 6. Mean density of CLT (12% MC).

Property	x_{mean}	*COV*
ρ_{glob} [kg/m^3]	462.60	5.19%
ρ_{withdr} [kg/m^3]	460.95	5.88%
$\rho_{sh\text{-}0°}$ [kg/m^3]	477.44	1.46%
$\rho_{sh\text{-}90°}$ [kg/m^3]	455.01	3.11%

Table 7. Characteristic density of CLT (12% MC).

Property	x_{char}
$\rho_{glob,05}$ [kg/m^3]	423.00
$\rho_{withdr,05}$ [kg/m^3]	416.25
$\rho_{sh\text{-}0°,05}$ [kg/m^3]	465.97
$\rho_{sh\text{-}90°,05}$ [kg/m^3]	431.70

Mechanical properties of the withdrawal tests are displayed in Tables 8-9. A typical load-displacement relationship (black line) and the trilinear approximating curve (red line) are presented in Figure 10.

Table 8. Mechanical properties of nail withdrawal tests.

Property	x_{mean}	*COV*
$K_{ser,ax}$ [N/mm]	1283.00	23.52%
u_y [mm]	1.73	24.18%
F_y [N]	2018.13	15.05%
u_{max} [mm]	2.41	12.82%
F_{max} [N]	2148.66	14.76%
u_{ult} [mm]	3.74	10.41%
F_{ult} [N]	1718.45	14.75%
Duct [-]	2.27	23.82%

Table 9. Characteristic withdrawal capacity of the nail.

Property	x_{char}
$F_{max,05}$ [N]	1604.94
$F_{max,95}$ [N]	2817.93

The symbols $K_{ser,ax}$ and $K_{ser,sh}$ signify, respectively, the slip moduli of the connection in the withdrawal tests and in the shear tests; the force and displacement at the yielding point are denoted as F_y and u_y; the maximum force and its displacement with F_{max} and u_{max}; and the ultimate force and its displacement with F_{ult} and u_{ult}. The ductility (Duct) was defined by the ratio between u_{ult} and u_y.

The withdrawal capacity of a nail depends upon the friction between the threaded shank and the timber. The force-displacement relationship in Figure 10 shows a linear fashion until the yielding point and a sudden reduction of bearing capacity after the displacement at which the maximum force is attained. Evident signs of failure were not visible either in the timber or in the nail.

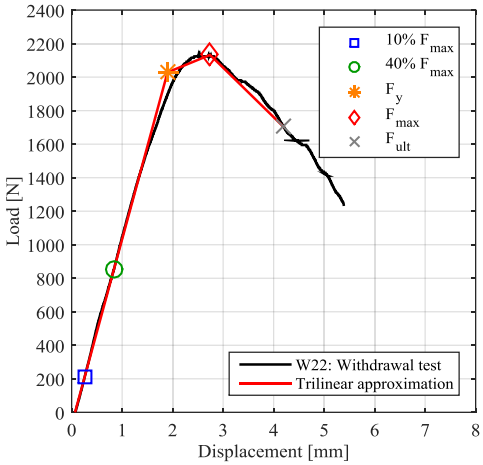

Figure 10. Force-displacement relationship and trilinear approximating curve of a nail withdrawal test.

The analytical model adopted by ETA-04/0013 (2013) defines the characteristic withdrawal capacity of a nail with threaded shank as:

$$F_{ax,Rk} = f_{ax,k} l_{thr} d \tag{3}$$

where l_{thr} = 44 mm is the threaded length of the shank, and $f_{ax,k}$ is the minimum between the values provided by Equation (4) and (5).

$$f_{ax,k} = 6.125\left(1+\frac{1.5d}{l_{thr}}\right)\left(\frac{\rho_k}{350}\right) \tag{4}$$

$$f_{ax,k} = \left(10.92 - 0.0158d - 0.0968 l_{thr}\right)\left(\frac{\rho_k}{320}\right)^2 \tag{5}$$

The withdrawal parameter $f_{ax,k}$ defined above was specifically calibrated on a threaded nail produced by Simpson Strong-Tie. Equation (3) was also adopted in Eurocode 5 (2014), however specific formulations for $f_{ax,k}$ were not included in the standard.

The analytical model of ÖNORM B 1995-1-1 (2014) was derived for a nail with a profiled surface driven in the plane side of a CLT panel; the withdrawal capacity depends upon the diameter d and the threaded length l_{thr} as shown in Equation (6).

$$F_{ax,Rk} = 14 d^{0.6} l_{ef} = 14 d^{0.6} l_{thr} \quad (6)$$

The characteristic nail withdrawal capacity in Table 9 and the analytical predictive models are compared in Table 10. The characteristic density presented in Table 7 ($\rho_{withdr,05}$) was used to define the withdrawal parameter in Equation (3).

Table 10. Comparison of characteristic experimental results and analytical values: Nail withdrawal tests.

Analytical model	$F_{ax,Rk}$ [N]	$\frac{F_{ax,Rk}}{F_{max,05}}$
ETA-04/0013	1456.88	0.91
ÖNORM	1415.20	0.88

Both models showed a good agreement with the experimental results; the analytical value of ETA-04/0013 (2013) is slightly higher than the one of ÖNORM B 1995-1-1 (2014), nevertheless discrepancies between models are less than 3%. However, it also should be mentioned that ÖNORM B 1995-1-1 (2014) suggests to use only 80% of $F_{ax,Rk}$ if the diameter of the nail is smaller than 6 mm.

Mechanical properties of the shear tests are summarized in Tables 11-12. Figure 11 presents a typical load-displacement relationship (black line) and the trilinear approximating curve (red line) of each test series.

Table 11. Mechanical properties of nail shear tests, parallel and perpendicular direction to face lamination of the panels.

Property	Parallel		Perpendicular	
	x_{mean}	COV	x_{mean}	COV
$K_{ser,sh}$ [N/mm]	483.69	17.81%	549.82	19.97%
u_y [mm]	7.63	27.67%	7.01	24.79%
F_y [N]	3508.51	5.39%	3916.14	9.66%
u_{max} [mm]	13.06	12.72%	12.90	9.83%
F_{max} [N]	3904.84	4.26%	4405.73	8.84%
u_{ult} [mm]	22.66	27.23%	15.59	14.75%
F_{ult} [N]	3275.26	4.32%	3877.99	12.06%
Duct [-]	3.13	37.95%	2.38	36.26%

Table 12. Characteristic lateral bearing capacity of the nail, parallel and perpendicular direction to face lamination of the panels.

Property	Parallel	Perpendicular
	x_{char}	x_{char}
$F_{max,05}$ [N]	3462.73	3549.46
$F_{max,95}$ [N]	4396.72	5435.40

The highest bearing capacity was reached in both directions at around 13 mm of displacement. Elastic stiffness and bearing capacity in perpendicular direction to the face lamination of the panels are 10-12% higher than in the parallel direction; on the contrary, ultimate displacement and ductility in the same direction are 30% lower than in the parallel direction.

Failures always occurred for tearing of the cap in one fastener due to a combination of nail withdrawal and bending (Figure 12). Two plastic hinges were recognised on all the fasteners tested, one under the cap and one another in the shank (10 to 15 mm below).

Timber panels tested in parallel to the face lamination (Figure 13-left) showed embedment failure in compression, while splitting was exhibited by some elements loaded in perpendicular direction (Figure 13-right).

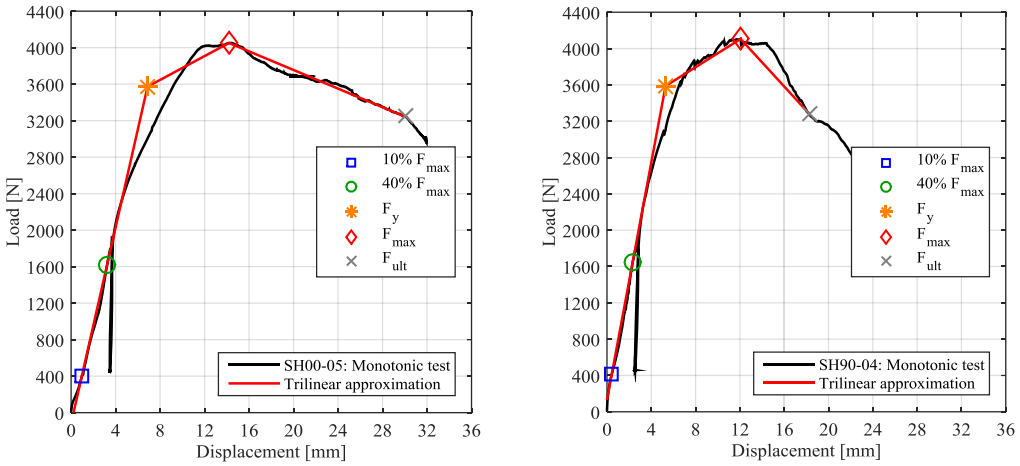

Figure 11. Force-displacement relationship with trilinear approximating curve of a nail shear test in parallel (left) and perpendicular (right) direction to the face lamination of the CLT panel.

Figure 12. Deformed fasteners after shear tests.

Figure 13. Damaged embedment after shear tests.

Eurocode 5 (2014) provides an equation for the prediction of the slip modulus of a steel-to-timber connection made with a nail without pre-drilling, depending upon the mean density of the panel ρ_m and the diameter d :

$$K_{ser} = 2\rho_m^{1.5} d^{0.8} / 30 \tag{7}$$

The experimental slip moduli defined in Table 11 and the analytical predictions obtained with Equation (7) are compared in Table 13. The mean values of density presented in Table 6 were used in the calculations (respectively $\rho_{sh\text{-}0°}$ and $\rho_{sh\text{-}90°}$).

Table 13. Comparison of experimental slip moduli and analytical predictions: nail shear tests in parallel and perpendicular direction to face lamination of the panels.

Analytical model	Parallel		Perpendicular	
	K_{ser} [N/mm]	$\frac{K_{ser}}{K_{ser,sh}}$	K_{ser} [N/mm]	$\frac{K_{ser}}{K_{ser,sh}}$
Eurocode 5	2108.32	4.36	1961.50	3.56
ÖNORM				

The analytical model prescribed by Eurocode 5 for steel-to-timber connections assumes a rigid metal plate; as visible in Table 13, however, the experimental results are significantly below the analytical values obtained with Equation (7), and it might be possible that this assumption was not fulfilled using a metal plate of 4 mm thickness, especially at low load levels.

ETA-04/0013 (2013) defines the characteristic lateral load-carrying capacity of a nail as:

$$F_{v,Rk} = F_{lat,Rk} + 0.6 F_{ax,Rk} \tag{8}$$

with $F_{ax,Rk}$ characteristic nail withdrawal capacity presented in Equation (3) and $F_{lat,Rk}$ lateral dowel capacity of a nail, defined as follows:

$$F_{lat,Rk} = \min \begin{cases} f_{h,k} t_1 d \\ f_{h,k} t_1 d \left[\sqrt{2 + \dfrac{4 M_{y,Rk}}{f_{h,k} t_1^2 d}} - 1 \right] \\ 2.3 \sqrt{M_{y,Rk} f_{h,k} d} \end{cases} \tag{9}$$

where the symbol t_1 denotes the penetration depth, assumed equal to 54 mm.

The rope effect is considered in Equation (8) separately from the lateral dowel capacity of the nail and its contribution is equal to 60% of the withdrawal capacity. On the contrary, the model included in Eurocode 5 (2014) and ÖNORM B 1995-1-1 (2014) defines the lateral load-carrying capacity of a nail as:

$$F_{v,Rk} = \min \begin{cases} f_{h,k} t_1 d \\ f_{h,k} t_1 d \left[\sqrt{2 + \dfrac{4 M_{y,Rk}}{f_{h,k} t_1^2 d}} - 1 \right] + \dfrac{F_{ax,Rk}}{4} \\ 2.3 \sqrt{M_{y,Rk} f_{h,k} d} + \dfrac{F_{ax,Rk}}{4} \end{cases} \tag{10}$$

Equation (10) considers a reduced contribution to the lateral capacity due to the rope effect, equal to 25% of the withdrawal capacity; moreover, the rope effect is neglected when the lateral load-carrying capacity is controlled by the embedment strength of the timber member.

The characteristic embedment strength in the timber member $f_{h,k}$ was defined in Eurocode 5 (2014) and ETA-04/0013 (2013) depending upon the characteristic density of the timber presented in Table 7 and the diameter of the fastener d :

$$f_{h,k} = 0.082 \rho_k d^{-0.3} \tag{11}$$

A specific formula for the embedment strength of a nail in a CLT member is defined in ÖNORM B 1995-1-1 (2014), as a function of the diameter of the fastener d :

$$f_{h,k} = 60 d^{-0.5} \tag{12}$$

The withdrawal capacity of Eurocode 5 (2014) and ETA-04/0013 (2013) were defined according to Equation (3), while Equation (6) was used for ÖNORM B 1995-1-1 (2014). Moreover, Equation (1) was adopted to define the yielding moment of the fastener, considering the diameter d and a ultimate tensile strength $f_{u,k}$ = 600 N/mm^2.

Table 14. Comparison of characteristic experimental results and analytical values: nail shear tests in parallel and perpendicular direction to face lamination of the panels.

Analytical model	Parallel		Perpendicular	
	$F_{v,Rk}$ [N]	$\frac{F_{v,Rk}}{F_{max,05}}$	$F_{v,Rk}$ [N]	$\frac{F_{v,Rk}}{F_{max,05}}$
ETA-04/0013	2857.20	0.83	2714.83	0.76
Eurocode 5	2286.39	0.66	2186.00	0.62
ÖNORM	2403.23	0.69	2403.23	0.68

The characteristic lateral bearing capacity and the analytical models are compared in Table 14. Conservative predictions were provided by all cases considered above, however ETA-04/0013 (2013) showed the best agreement with the experimental results. Discrepancies among the values shown in Table 14 are related to the different approaches followed by the standards to account for the rope effect.

5 NUMERICAL MODEL AND ANALYSES

The experimental results presented in Section 3 were used to calibrate a numerical model of a nail driven in the plane side of a CLT panel. The nailed connection was simulated with three non-linear spring elements (Rinaldin *et al.* 2013).

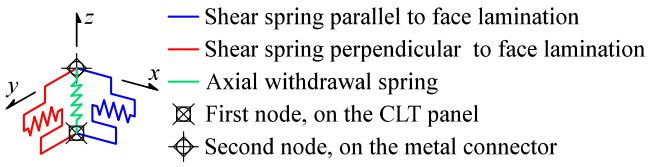

Figure 14. Numerical model of a nail in a CLT panel.

Each non-linear spring is connected on one side to the CLT panel (first node) and on the other side (second node) to the metal connector (Figure 14). Two hysteresis laws have been adopted, to characterize the behaviour of the connection under shear and withdrawal loads.

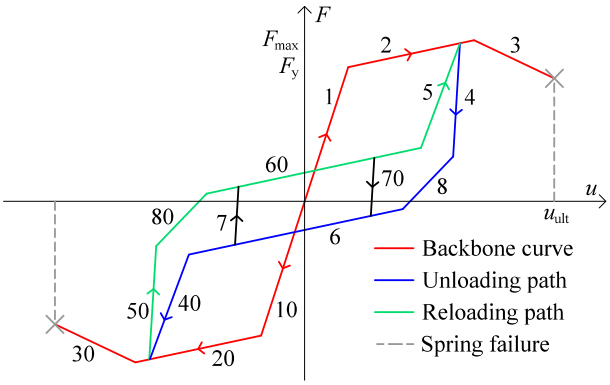

Figure 15. Piecewise-linear law for shear springs (Rinaldin *et al.* 2013).

The piecewise-linear law used to characterize the shear springs (red and blue spring in Figure 14) is symmetric and is made of 16 branches. As visible in Figure 15, the backbone curve has an elastic branch up to yielding and two inelastic branches up to failure, the first with hardening and the second with softening. If the nail is unloaded, branch #4 is followed until a given percentage of the force on the backbone curve is reached (chosen with a specific input parameter).

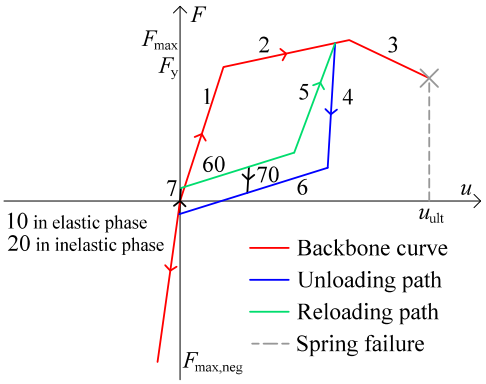

Figure 16. Piecewise-linear law for withdrawal spring (Rinaldin *et al.* 2013).

The piecewise-linear law of the withdrawal springs (Figure 16) is made of 11 branches and considers hysteresis loops in tension and contact behaviour in compression. The backbone curve is not symmetric: an elastic branch followed by two inelastic branches are considered in tension, while an elastic behaviour up to the maximum force is adopted in compression (branches #10 and #20 are overlapped).

Typical features of timber connections such as stiffness and strength degradation were not considered at this stage of the research and will possibly be introduced in future studies.

As an applicative example, monotonic shear and tension tests were simulated on a FE model of a Simpson Strong-Tie AE116 angle bracket. Both metal connector and the first board layer of the CLT panels were accounted in the model and meshed using, respectively, 10-node tetrahedron elements and 15-node triangular prism elements (C3D10 and C3D15). Timber panels do not affect the

mechanical behaviour of the connector, and were introduced to account for the surface-to-surface contact interaction. Steel was modelled as an elastic-plastic material (E = 210 GPa, ν = 0.3 and f_y = 230 MPa), while an equivalent-elastic isotropic material was adopted for timber (with E = 600 MPa and ν = -0.57).

Twenty-one nails anchor the angle bracket to the external surfaces of the CLT panels, where the boundary conditions are also applied. Fourteen nails are located in the long leg and seven in the short leg (pattern B of ETA 06/0106 2013); the spring elements discussed above were used to simulate the non-linear behaviour of the nails.

Figure 17 presents a deformed view of the system after the shear and tension tests, while Tables 15-16 present a comparison between the experimental properties and the numerical results (x_{exp} and x_{FEM}). Significant discrepancies were observed between numerical and experimental results, and further studies are required to improve the performances of the model. Cold forming might have had an influence on the bearing capacity, especially under tension loads. Moreover, results might have been affected by a unique definition of the mechanical properties of the nails instead of considering a typical scatter of values.

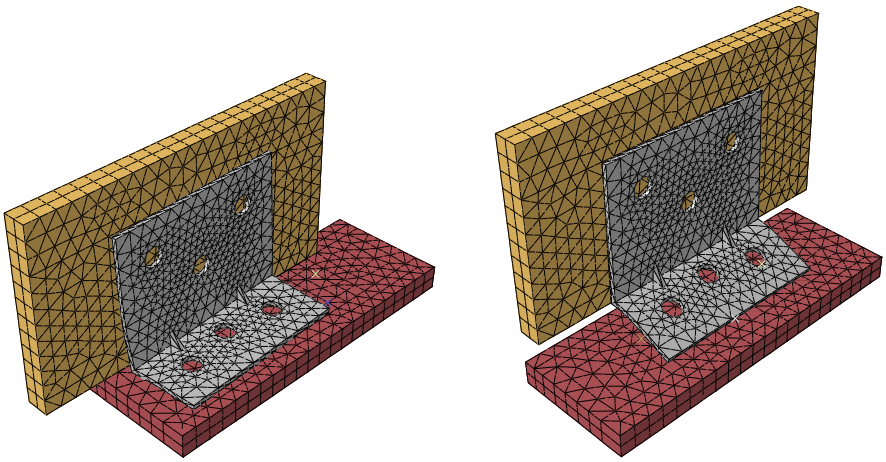

Figure 17. FE model of a Simpson Strong-Tie AE116 angle bracket: shear test (left) and tension test (right).

Table 15. Comparison of experimental properties and numerical results: Shear test.

Property	x_{exp}	x_{FEM}	$\frac{x_{exp}}{x_{FEM}}$
$K_{ser,sh}$ [N/mm]	2872.57	1811.61	1.59
F_{max} [kN]	22.41	26.77	0.84

Table 16. Comparison of experimental properties and numerical results: Tension test.

Property	x_{exp}	x_{FEM}	$\frac{x_{exp}}{x_{FEM}}$
$K_{ser,ax}$ [N/mm]	19050.95	2616.42	7.28
F_{max} [kN]	13.07	9.19	1.42

Numerical simulations were also performed under cyclic conditions, however not negligible differences were observed between numerical results and experimental properties, and additional work is required.

6 CONCLUSIONS

An experimental programme was performed on Simpson Strong-Tie annular ringed shank nails, used in CLT buildings to anchor the metal connectors to the timber panels. Monotonic shear tests in parallel and perpendicular direction to the face lamination of a CLT panel, and withdrawal tests, were carried out to investigate the bearing capacity of a nail driven in the plane side of a CLT panel. Furthermore, tension tests and bending tests were performed on single fasteners to determine, respectively, the ultimate tensile strength and the yielding moment of the nails. Mean and characteristic values of the mechanical properties were obtained and compared with the analytical formulations provided by the reference standards (EN 1995-1-1:2004+A2; ETA-04/0013; ÖNORM B 1995-1-1). ETA-04/0013 showed the best agreement with the experimental results, both for the lateral and the withdrawal load-carrying capacity of the connection. Due to the different approach used to account for the rope effect, EN 1995-1-1:2004+A2 and ÖNORM B 1995-1-1 provided conservative predictions of the lateral load-carrying capacity, on the contrary, the experimental slip moduli are significantly low compared with the analytical model prescribed in the standards.

The experimental results were used afterwards to calibrate a FE model of a nail driven in the plane side of a CLT panel. As a first applicative example, monotonic shear and tension test were simulated on a FE model of a Simpson Strong-Tie AE116 angle bracket (ETA 06/0106 2013), and compared with analogous setups tested by the holz.bau forschungs gmbh. The significant discrepancies might be related to the assumptions on which the numerical model was derived, and further studies are required. The use of these numerical models would limit the need of experimental testing to a minimum, and would allow the prediction of the monotonic and cyclic behaviour of a certain metal connector where some elements (e.g. the number of nails or the position of the connector in the wall systems) were changed with respect to the setup tested. Moreover, these models could be used to predict the performances of the metal connectors in situations that cannot be easily tested, such as the simultaneous application of axial and shear loads.

Future studies will focus on the lateral bearing capacity of a nail in the plane side of a CLT panel under fully reversed cyclic loads. Moreover, additional bending tests will be performed to investigate the bending behaviour of single fasteners under cyclic loads. Finally, future investigations will improve the performances of the numerical models, solving the issues arisen at the current stage of the research.

7 FUTURE COLLABORATION AND FORESEEN PUBLICATIONS

The results obtained within the current STSM have been collected in a conference paper and submitted for oral presentation to the XVI Conference of the Italian National Association of Earthquake Engineering (ANIDIS 2015, L'Aquila, Italy). The paper is entitled "Experimental tests on annular ringed shank nails for seismic resistant Cross-Laminated Timber (CLT) structures" and is authored by Izzi M., Flatscher G., Rinaldin G., Fragiacomo M. and Schickhofer G.

A second conference paper is scheduled to be submitted for oral presentation to the XIV World Conference on Timber Engineering (WCTE 2016, Vienna, Austria). Mean and characteristic values

of the mechanical properties of the cyclic shear tests in parallel and perpendicular direction to the face lamination of the CLT panels will be presented and critically discussed. Moreover, overstrength factors will be obtained in accordance with the current standards.

Finally, a journal article will be submitted for publication before December 2015.

8 AKNOWLEDGEMENTS

The author gratefully acknowledges COST FP1402 and FP1004 Management Committees and the representatives of COST Office for the STSM grants, which contributed to a successful outcome of this research. The local host Professor Gerhard Schickhofer, the Ph.D. Candidate Georg Flatscher, and the holz.bau forschungs gmbh are gratefully acknowledged for giving access to the laboratory and all the facilities provided by the Institute of Timber Engineering and Wood Technology, for sharing the test data of the COMET Project "focus_sts" SGSC 3.1.1_1, and for the advices, help and collaboration throughout the STSMs.

9 REFERENCES

Bratulic, K., Flatscher G. and Brandner R. (2014). Monotonic and cyclic behavior of joints with self-tapping screws in CLT structures. *COST Action FP1004, Experimental Research with Timber*, Prague, Czech Republic, pp. 1-8.

Ceccotti, A., Lauriola M. P., Pinna M. and Sandhaas C. (2006). SOFIE project-cyclic tests on cross-laminated wooden panels. *Proceedings of the 9th World Conference on Timber Engineering (WCTE)*, Portland, Oregon, USA.

Ceccotti, A. (2008). New technologies for construction of medium-rise buildings in seismic regions: the XLAM case. *Structural Engineering International* **18**(2): 156-165, doi: http://dx.doi.org/10.2749/101686608784218680.

Ceccotti, A., Sandhaas C., Okabe M., Yasumura M., Minowa C. and Kawai N. (2013). SOFIE project-3D shaking table test on a seven-storey full-scale cross-laminated timber building. *Earthquake Engineering & Structural Dynamics* **42**(13): 2003-2021, doi: http://dx.doi.org/10.1002/eqe.2309.

Ehlbeck, J. and Larsen H. (1993). Eurocode 5-Design of timber structures: joints. *International Workshop on Wood Connectors*, Forest Product Society, pp. 9-23.

EN 384 (2010). Structural timber. Determination of characteristic values of mechanical properties and density. CEN, Brussels, Belgium.

EN 409 (2009). Timber structures. Test methods. Determination of the yield moment of dowel type fasteners. CEN, Brussels, Belgium.

EN 1380 (2009). Timber structures. Test methods. Load bearing nails, screws, dowels and bolts. CEN, Brussels, Belgium.

EN 1995-1-1:2004+A2 (2014). Eurocode 5: Design of timber structures. General. Common rules and rules for buildings. CEN, Brussels, Belgium.

EN 12512:2001/A1 (2005). Timber structures. Test methods. Cyclic testing of joints made with mechanical fasteners. CEN, Brussels, Belgium.

EN 14358 (2006). Timber structures. Calculation of characteristic 5-percentile values and acceptance criteria for a sample. CEN, Brussels, Belgium.

EN 26891 (1991). Timber structures. Joints made with mechanical fasteners. General principles for the determination of strength and deformation characteristics. CEN, Brussels, Belgium.

ETA-04/0013 (2013). European Technical Approval. CNA Connector nails, PCR Connector nails and CSA Connector screws. European Organisation for Technical Approvals, Brussels, Belgium.

ETA-06/0106 (2013). European Technical Approval. Three-dimensional nailing plate (timber-to-timber/timber-to-concrete angle bracket). European Organisation for Technical Approvals, Brussels, Belgium.

Flatscher, G., Bratulic K. and Schickhofer G. (2014a). Screwed joints in cross-laminated timber structures. *Proceedings of the 13th World Conference on Timber Engineering (WCTE)*, Quebec City, Quebec, Canada.

Flatscher, G., K. Bratulic and G. Schickhofer (2014b). Experimental tests on cross-laminated timber joints and walls. *Proceedings of the ICE - Structures and Buildings*, 10 pp., doi: http://dx.doi.org/10.1680/stbu.13.00085.

Flatscher, G. and Schickhofer G. (2015). Shaking table test of a cross-laminated timber structure. *Proceedings of the ICE - Structures and Buildings* (accepted, in press).

Gavric, I., Fragiacomo M. and Ceccotti A. (2013). Capacity seismic design of X-Lam wall systems based on connection mechanical properties, CIB-W18/46-15-2. *Proceedings of the 46th CIB-W18 Meeting*, Vancouver, Canada.

Gavric, I., Fragiacomo M. and Ceccotti A. (2015a). Cyclic behaviour of typical metal connectors for cross laminated timber (CLT) structures. *Materials and Structures* **48**(6): 1841-1857, doi: http://dx.doi.org/10.1617/s11527-014-0278-7.

Gavric, I., Fragiacomo M. and Ceccotti A. (2015b). Cyclic behavior of typical screwed connections for cross-laminated (CLT) structures. *European Journal of Wood and Wood Products* **73**(2): 179-191, doi: http://dx.doi.org/10.1007/s00107-014-0877-6.

Gavric, I., Fragiacomo M. and Ceccotti A. (2015c). Cyclic behavior of CLT wall systems: Experimental tests and analytical prediction models. *Journal of Structural Engineering* 04015034, 14 pp., doi: http://dx.doi.org/10.1061/(ASCE)ST.1943-541X.0001246.

Hummel, J., Flatscher G., Seim W. and Schickhofer G. (2013). CLT wall elements under cyclic loading - details for anchorage and connection. *COST Action FP1004, Focus solid timber solutions, European Conference on Cross Laminated Timber (CLT)*, Graz, Austria, pp. 152-165.

Lauriola, M. P. and Sandhaas C. (2006). Quasi-static and pseudo-dynamic tests on XLAM walls and buildings. *COST Action E29, International Workshop on Earthquake Engineering on Timber Structures*, Coimbra, Portugal, pp. 119-133.

ÖNORM B 1995-1-1 (2014). Bemessung und Konstruktion von Holzbauten: Allgemeines. Allgemeine Regeln und Regeln für den Hochbau. Nationale Festlegungen zur Umsetzung der ÖNORM EN 1995-1-1 nationale Erläuterungen und nationale Ergänzungen. ÖN, Wien, Austria.

Rinaldin, G., Amadio C. and Fragiacomo M. (2013). A component approach for the hysteretic behaviour of connections in cross-laminated wooden structures. *Earthquake Engineering & Structural Dynamics* **42**(13): 2023-2042, doi: http://dx.doi.org/10.1002/eqe.2310.

Tomasi, R. and Smith I. (2014). Experimental Characterization of Monotonic and Cyclic Loading Responses of CLT Panel-To-Foundation Angle Bracket Connections. *Journal of Materials in Civil Engineering* 04014189 **27**(6), 10 pp., doi: http://dx.doi.org/10.1061/(ASCE)MT.1943-5533.0001144.

Uibel, T. and Blaß H. J. (2006). Load carrying capacity of joints with dowel type fasteners in solid wood panels, CIB-W18/39-7-5. *Proceedings of the 39th CIB-W18 Meeting*, Florence, Italy.

Uibel, T. and Blaß H. J. (2007). Edge joints with dowel type fasteners in cross laminated timber, CIB-W18/40-7-2. *Proceedings of the 40th CIB-W18 Meeting*, Bled, Slovenia.

10 APPENDIX

Confirmation by the host institute of the successful outcome of the STSM.